STATISTICS, OPTIMIZATION AND INFORMATION COMPUTING
Stat., Optim. Inf. Comput., Vol. **14**, July 2025, pp 144–161.
Published online in International Academic Press (www.IAPress.org)

Ensemble Method for Intervention Analysis to Predict the Water Resources of the Tigris River

Muzahem Al-Hashimi*, Heyam Hayawi, Mohammed Alawjar

Department of Statistics and Informatics, University of Mosul, Iraq

Abstract Iraq faces real challenges and great concerns regarding water resources, including the noticeable decrease in the flow of the Tigris River into Iraqi territory due to various irrigation projects being implemented on the Turkish side, the latest of which was the construction of the Ilisu Dam, which exacerbated the water crisis and placed Iraq before a serious challenge. The flow river data utilized in this paper was the annual revenue of the Tigris River, representing the amount of water entering Iraq at the Turkish border data for the period (Oct-2014–Sep-2021), which equals 84 months. To enhance the accuracy of Tigris River flow forecasting with the ARIMA models as a classical statistical approach and the nonlinear model of eXtreme Gradient Boosting (XGBoost), a Random Tree ensemble model was proposed in this study. Two distinct ARIMA models are employed to capture the linear characteristics of the Tigris River flow: SARIMA and ARIMAX. XGBoost model was utilized to capture the nonlinear characteristics of the Tigris River flow. The results reveal that the Tigris River flow prediction using the Random Tree ensemble model achieves better than the other models introduced in this paper regarding the evaluation measurements. The forecast suggests stabilizing the river flow aligning with the low average river flow level, with variations observed. These seasonal changes reflect the impact of increased river flow during the rainy season in Iraq and Turkey during peak times and reduced river flow in the summer months.

Keywords Tigris River Flow, SARIMA, ARIMAX, XGBoost, Ensemble Model, Random Tree

DOI: 10.19139/soic-2310-5070-2413

1. Introduction

1.1. The Ilisu Dam: Challenges for the Tigris River Flow

It is an objective fact that Iraq is facing real challenges. These include climate change, rising temperatures, the accompanying drought and lack of rain, and a noticeable decrease in the discharge of the Tigris River into Iraqi territory due to reservoir and dam projects built in Turkey. The situation has worsened significantly with Turkey's construction of the Ilisu Dam on the Tigris River, which has led to a clear shortage in Iraq's share of water.

The Tigris River originates from Lake Van in the southeastern highlands of Turkey. It enters the Iraqi border in the northern part of the Fishkhabur area, heads southeast, and continues until it intersects with the Euphrates at al Qurna in Iraq's southern region, ultimately emptying into the Arabian Gulf. It has a length of 1,400 km within the Iraqi border out of 1900km [1]. Among its tributaries are the Khabur and the Upper Zab, which originate in Turkey and Iraq; the Lower Zab and Diyala, which originate in Iran and Iraq; and the Azim, which originates in Iraq [1]. The Tigris River and its tributaries from Turkiye feed eight of the 18 governorates: Dohuk, Nineveh, Salah al-Din, Baghdad, Wasit, Maysan, and Basra. The population benefiting from the main Tigris River and its tributaries coming from Turkey is about 25 million people, which is approximately 58% of the population of Iraq for the year 2023.

*Correspondence to: Muzahem Al-Hashimi (Email: muzahim_alhashime@uomosul.edu.iq).
Department of Statistics and Informatics, University of Mosul, Mosul, Iraq.

ISSN 2310-5070 (online) ISSN 2311-004X (print)

Figure 1. Ilisu Dam (Source: Google Earth, accessed on Jun 15, 2025)

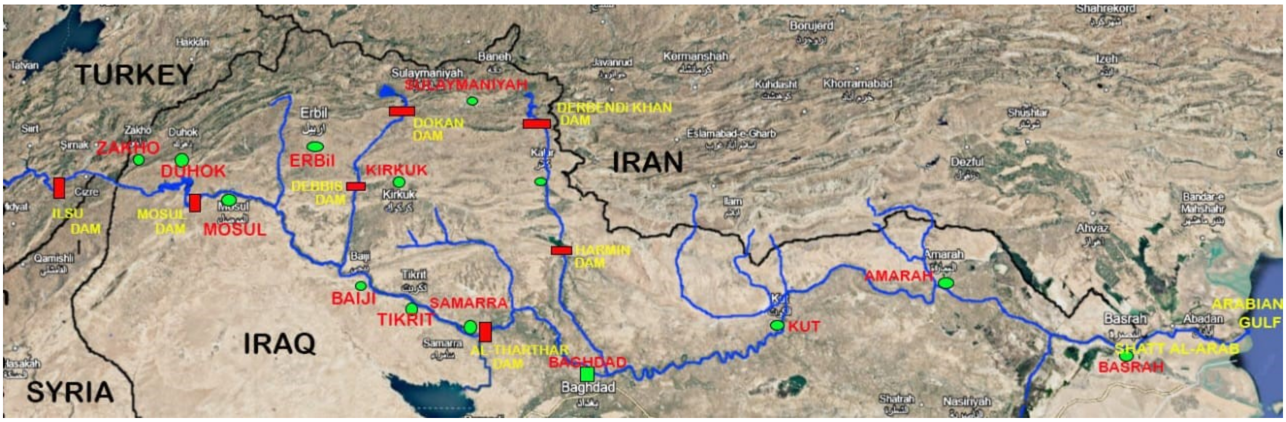

Figure 2. Tigris River basin

The Tigris River is vital in Iraq, providing most of the nation's water resources. The annual revenues of the Tigris River were estimated at (30.87, 21.13, 32.3, and 9.05) billion/m3, representing (71.34%, 68.58%, 62.00%, and 56.50%) of the total annual revenues of the Tigris and Euphrates Rivers, which were estimated at (43.27, 30.69, 52.1, and 16.02) billion/m3 for the years 1990-1991, 2000-2001, 2010-2011, and 2022-2023 respectively [1, 2].

The Tigris River Basin is a trans boundary communal area in four countries (Turkey, Syria, Iraq, and Iran). Since 1941, the Tigris River and its tributaries have had fourteen barrages and dams due to the competition over shared water resources [3, 4, 5, 6].

The Ilısu Dam is a component of the Southeastern Anatolian Project initiated in 1977. It is the longest concrete-face rock-fill dam in the world, situated in Siirt, Batman, and Diyarbakır provinces. It was constructed within the boundaries of Ilısu village, Dargeçit County, between Mardin and Şırnak on the Tigris River, 65 km upstream from the Syrian-Iraqi border, perched at a height from the valley 135 m, a length of 1,820 m with the volume of 43,800,000 m3. It was completed in 2017 [7, 8, 9]. The Dam is designed to accommodate 10.41 Billion cubic meters in its reservoir and is aimed at power generation and irrigation [Rahi, K.A. and Halihan, T., 2018]. Ilisu Dam will operate alongside Cizre Dam, which is currently in the planning phase and will be positioned 45 km downstream from Ilisu Dam, around 20 km upstream near the Iraq-Syria border [9]. They aim to generate power and irrigation by channeling water east of the main river course [10].

1.2. An Overview of Related Methods

Forecasting river flow plays a key role in developing water resource projects, enhanced utilization of water resources, crop irrigation infrastructure, and water-powered energy systems. With ongoing population growth, uses in industry, and watering requirements, it has become a major focus for researchers working on effective river management [11, 12, 13, 14].

Many variables influence the unpredictable direction of water flows. Therefore, effective forecasting of water flows is very difficult due to highly variable climate change and unpredictable policies of riparian countries.

The family ARIMA techniques have been the most widely used in the field of Hydrology for more than three decades, encompassing river flow prediction [11, 15, 16, 17]. This property is due to its ease of implementation and interpretation, where the estimation of the system is linearly and has a lower number of parameters [18, 19].

Papamichail and Georgiou [20] utilized the SARIMA models to forecast inflows for the planned Almopeos Reservoir in Greece. Ghanbarpour et al. [21] used the ARIMA model to forecast karstic flow in the Karkheh subbasin of southwest Iran. Valipour, M. et al., [22] employed ARMA and ARIMA models to forecast the inflow of the Dez dam reservoir. Bazrafshan O. et al., [23] applied the ARIMA and SARIMA models to forecast the Karkheh Basin standard runoff Index in the Karkheh Basin. Valipour [24] used SARIMA and ARIMA models to assess long-term runoff forecasting in the United States. Ullah and Hussain [25] used the SARIMA model to forecast water outflow at the Indus River at Terbela. De Sousa et al. [26] used the ARIMA statistical model to forecast water flow and sediment flux. Musarat et al. [27] adopted the ARIMA model to forecast the Kabul River water level. Pires and Martins [28] utilized the ARIMA model to forecast water flow in public supply systems in the medium term.

ARIMA models face several major constraints. For instance, it is complicated to represent nonlinear relationships accurately, stationary requiring time series [11], and accurate results require a large amount of historical data [29]. ARIMA assumptions often conflict with the complex nonlinear patterns found in the dominant pattern of time series data [30, 31]. Therefore, several machine-learning and hybrid techniques have recently been devised to meet the challenges associated with forecasting models.

El-Shafie et al. [32] used the ANFIS model to forecast the monthly inflow of the Nile River at the Aswan High Dam. Huang [33] Forecasting flows in Apalachicola River using artificial neural networks (ANN). Altunkaynak [34] used ANN to model and predict the temporal fluctuations of Lake Van water levels in Turkey. Wu and Chau [35] predict monthly streamflow time series across diverse areas in China by using K-Nearest-Neighbors, and ANN, Phase Space Reconstruction (ANN-PSR), and Moving Average Artificial Neural Networks (MA-ANN). Shabri and Suhartono [36] applied the Least-Squares Support Vector Machine Model, ANN, SVM, and ARIMA for forecasting streamflow forecasting Kinta River in Perak, Peninsular Malaysia. Kalteh [37] forecasts monthly river flow for Kharjegil and Ponel in Northern Iran using (ANN) and support vector regression models coupled with wavelet transform. Bhagwat and Maity [38] hydroclimatic streamflow prediction using least square-support vector regression. He et al. [39] forecast river flow in small river basins within semiarid mountain regions using ANN, adaptive neuro-fuzzy inference system (ANFIS), and support vector machine (SVM). Kisi et al. [40] used three machine learning models, Multivariate Adaptive Regression Splines, M5 Model Tree, and Least Squares Support Vector Machine to predict streamflow in the Mediterranean region of Turkey. Tosunoğlu et al. [41] used Support Vector Machines, Adaptive Boosting, K-nearest neighbors, and Random Forests to model monthly streamflow in the Coruh River basin in Turkey. Sharma et al. [42] utilized Data-Driven Models and Model Tree for streamflow forecasting in the Purna River in the Tapi Basin, India. Chebii et al. [43] utilized Artificial Neural Network to predict floods in River Perkerra in Kenya's Rift Valley region. Reed [44] applied Convolutional Long Short-Term Memory (ConvLSTM) Networks, Convolutional Neural Networks (CNNs) for Active Learning, Transfer Learning, and Persistence Model for flow prediction in the South Platte River, Colorado, in the United States. Maiti et al. [45] used deep learning models along with SARIMA for river flow forecasting Periyar River in South India. Wang et al. [46] used Support Vector Machine with Radial Basis Function, Support Vector Machine with Polynomial Kernel, Decision Tree, Gradient Boosting, Random Forest, Long Short-Term Memory, and Multiple Linear Regression. Furthermore, hybrid models combine machine-learning techniques with wavelet theory to compute monthly streamflow estimates for the Snake River in Idaho, USA

Water is a necessity that makes up the world and the nation's environmental well-being, where the demand for

the spread of irrigated agriculture increases, the economy grows, and the population expands. This is offset by a reduction in water availability, which increases pressure on water flow. The water flow fluctuations are generally affected by climate fluctuations and varying seasonal conditions, and unpredictable rainfall patterns lead to floods or exacerbate water scarcity. To predict water flow changes, researchers differ in achieving the best forecasts with the least possible error. Decision-makers and farmers look at managing water resources in light of accurate forecasts, especially regarding the uncertainty of climate and water flows from neighboring countries. Predicting future water flows is very important to decision-makers and agricultural producers alike. Accurate forecasts of the future help develop effective policies to support stability and development in countries, make wise decisions, and negotiate everything that supports water flow stability in riparian countries.
Water flow is intricate and involves a variety of unpredictable elements. Accurately defining it as either linear or nonlinear is challenging. Therefore, models for Tigris River flow forecasting must account for linear and nonlinear features. This study proposes a predictive model that effectively captures the Tigris River flow behavior, identifies the significant patterns using an ensemble method, and forecasts up to October 2026. The study's knowledge can help decision-makers review and provide insights for water policy formulation.

2. Modeling Techniques for Time Series Analysis

2.1. Time Series

A time series is a set of observations about a phenomenon taken in a certain chronological order, usually with equal time intervals [47]. What distinguishes it is the correlation between its observations, mathematically defined as a sequence of random variables defined within the multivariate probability space and indicated by the evidence t, which belongs to the evidence group T and symbolizes the time series usually $\{Y(t), t \in T\}$. There are two types of time series: Discrete and continuous [48].

Time series are used to analyze patterns and predict future trends. For example, time series can be used to track stock prices, temperatures, or product sales. A time series is said to be stationary if it satisfies the following properties [49]:

- The mean $E(Y_t)$ is the same for all t.
- The variance of Y_t is the same for all t.
- The covariance between Y_t and Y_{t-h} is the same for all t at each lag $h = 1, 2, 3, \ldots$.

The Autocorrelation Function (ACF) is equal:

$$\rho_{Y_t, Y_{t-h}} = \frac{\text{Covariance}(Y_t, Y_{t-h})}{\text{Std.Dev.}(Y_t) \cdot \text{Std.Dev.}(Y_{t-h})} = \frac{\text{Covariance}(Y_t, Y_{t-h})}{\text{Variance}(Y_t)}$$

Many techniques can applied to analyze time series, such as moving averages to analyze trends or statistical models such as ARIMA to predict future values.

2.2. Intervention Analysis

Intervention time series analysis developed by [50]. It is widely used to address the impact of interventions on the time series regression framework. Intervention is an external event that affects the time series, as it changes the average of the time series and leads to its sudden deviation, so it is a special model of time series models [50]. Examples of Intervention are natural disasters such as earthquakes, storms, floods, or drought, epidemics such as the beginning of a pandemic (such as COVID-19) or the outbreak of war, or it may be economic recovery or economic boom. There are two intervention variables: a step variable, which takes the value 1 when the event occurs and continues, and zero for other times. The pulse variable, also called a point variable, is a binary variable represented only once, taking the value 1 for a single point in time and zero for absence [50].

2.3. Extreme gradient boosting (XGBoost)

Chen and Guestrin (2016) [51] proposed XGBoost as a more sophisticated gradient-boosting algorithm encompassing system improvement and methodology enhancement. XGBoost is an ensemble decision-tree-based machine-learning algorithm that provides flexibility and efficiency and is used for regression and classification [52]. It is an ensemble of weak learners to create a powerful classifier in a linear way, which is handled by each successive decision-tree learning based on the errors of the preceding decision-tree in sequence [51]. For a dataset of size n samples, there are response variables y_i, and explanatory variables x_i have k features. The tree ensemble model implemented in the XGBoost is trained iteratively in an additive-step process to estimate the response variable, based on the explanatory variables and the number of regression functions (m):

$$\hat{y}_i = \sum_{m=1}^{M} f_m(x_i), \quad f_m \in F$$

Where F represents the space of all potential trees. The aim is to minimize the regularized objective as follows,

$$L(\Phi) = \sum_{i=1}^{n} l(\hat{y}_i, y_i) + \sum_{m=1}^{m} \Omega(f_m)$$

Where l is the loss function for base learners to define and optimize the objective function, and Ω is the regularization term that constrains the model's complexity to mitigate overfitting [53]. XGBoost utilizes parameters to determine an optimal tree structure by applying the greedy search algorithm [54].

2.4. Ensemble model

Ensemble forecasting is a technique that involves integrating multiple data sources and model types, leveraging varying assumptions and methodologies to identify patterns. The aim is to maximize the use of all relevant data for predictions, avoiding the constraints and arbitrary decisions tied to adopting only one method or machine learning technique, a specific functional form, or a restricted dataset [55]. Rather than delivering a single outcome, ensemble model outputs present a spectrum of possible outcomes from various base models. This method typically improves both accuracy and robustness in forecasting. Three main reasons can explain the strengths of combining models for time series forecasting. Using appropriate aggregation methods markedly improves overall forecasting accuracy. Combination strategies are the best choice when there is considerable uncertainty regarding the optimal forecast model. The integration of various forecasts is an efficient way to reduce errors [49, 55, 56, 57].

2.5. Random Tree

Random Tree is a supervised machine-learning technique popular in data mining that Leo Breiman and Adele Cutler introduced. This algorithm is designed to be applied to both classification and regression problems. It's an ensemble learning technique that generates a variety of individual models. These are composed of a collection of single decision trees and random forests as part of the machine learning methodology. Two ways of randomization generate tree diversity. It utilizes the bagging concept to create a random subset of data for decision tree generation. In a conventional decision tree, nodes are split by choosing the best division from all available variables [58, 59].

2.6. Hyperparameters in Machine Learning

Hyperparameters are vital to the performance of the Machine learning algorithms. Given their direct role in affecting the model, they enhance computational performance, manage overfitting, and address class imbalance. A commonly implemented tuning technique is Grid search, which builds upon each model's hyperparameters and iteratively adjusts each hyperparameter of the specified model to pinpoint the optimal parameters [56, 60, 61].

2.6.1. Hyperparameters in XGBoost There are seven fundamental hyperparameters in XGBoost, including "max-depth" that controls the depth limit for each decision tree. "Minimum child weight" that it specifies the minimum weight sum necessary in a leaf (child), which assists in reducing overfitting. “gamma” it lowers the threshold for loss reduction needed to create a split; increasing gamma leading to less overfitting and a more conservative model. “subsample” it regulates the fraction of training data used per boosting iteration. “colsample by tree” it defines the proportion of columns sampled when constructing a tree. “alpha for L1 regularization” contributes to simplifying the model and improving its efficiency which can reduce overfitting, and “learning rate” that regulates the step size and shrinkage as boosting progresses [62, 63].

2.6.2. Hyperparameters in Random Tree There are four fundamental hyperparameters in Random Tree, including “max-depth”, which defines the depth limit for the trees. “Maximum Features” it’s the selected features for each node split as the tree is being constructed. ‘Minimum samples per split” refers to the minimum samples needed to split a node as the tree is being constructed. ‘Minimum samples per leaf” refers to the minimum samples needed in a leaf as the tree is being constructed [64].

3. Data Sources and Preparation

The flow river data utilized in this paper was the annual revenue of the Tigris River, representing the amount of water entering Iraq at the Turkish border data for the period (Oct-2014–Sep-2021), which equals 84 months. The data was downloaded from the Environmental Statistics of Iraq- Water Quantity and Quality from the Central Statistical Organization. Tigris river flow data is defined as the water inflow of the amount of surface water of the Tigris River passing through the Tigris River at an Iraq station of Fishkhabour at the Iraq-Turkish border during the water year, in units of measurement (billion m3/year). The water year in Iraq starts from October 1 of each year until September 30 of the following year. The data was prepared before it was used to ensure the accuracy of future predictions of Tigris River flow in Iraq, including handling missing values using Mean Imputation. For model development and evaluation, the data was split into a training set for the data before Jan 2020 to develop the model and a testing set for data from Jan 2020 to May 2021 to test its effectiveness. Scaling was applied to improve model convergence for both training and testing data. The ARIMA models were implemented using SAS 9.4 and MINITAB 22.1, XGBoost implemented using Python (Jupyter Notebook), and Random tree ensemble model implemented using Weka 3.8.2.

4. Results and Discussion

4.1. Data Description and Exploratory Analysis

The Tigris River Basin is one of the large basins shared between four riparian countries: Iran, Iraq, Syria, and Turkey. The basin area encompasses 221,000 km², with Iraq contributing 56.1%, Turkey 24.5%, Iran 19%, and Syria 0.4% [Haghighi et al., 2023]. There are 14 main dams within the basin, with a combined maximum storage capacity of 116.5 BCM. The projected irrigated area in the basin is 4.6 million hectares, while the projected irrigated area outside the basin is 150,000 hectares [Haghighi et al., 2023].

Descriptive statistics provide a comprehensive overview of the monthly water flow of the Tigris River in Iraq. There were 84 observations representing the flow of the Tigris River, which was recorded as it entered the border between Turkey and Iraq. The observations encompass water flow data across various ranges. The maximum recorded value was 2837 m³/second in April 2019, while the lowest was 79 m³/second in October 2017. The mean water flow was 480.70 m³/second, suggesting a central tendency measure reflecting the average tendency of a dataset. The median was 380 m³/second, offering additional insights into the water flow and highlighting potential outliers. The mode of water flow was 206 m³/second (October 2014 and July 2015), 261 m³/second (January 2017 and August 2019), 278 m³/second (November 2014 and February 2020), and 321 m³/second (July 2019 and Jun 2020). Representing the most common occurrence, illuminating a specific water flow point that frequently occurred, helping to identify key trends or patterns in the data, or indicating impactful factors in particular periods.

The standard deviation was 455.1 m³/second of the points, representing the variation of individual data points from the mean.

Fig. 3 demonstrates the Tigris River's behavior regarding the water flow in Iraq from Oct. 2014 to Sep. 2021. The Tigris water flow series before the Ilisu Dam intervention ranged from Oct. 2014 to Apr. 2019, while after the Ilisu Dam intervention ranged from May 2019 to Sep. 2021. Tigris water flow demonstrated a notable downward trajectory with the dam running in 2019.

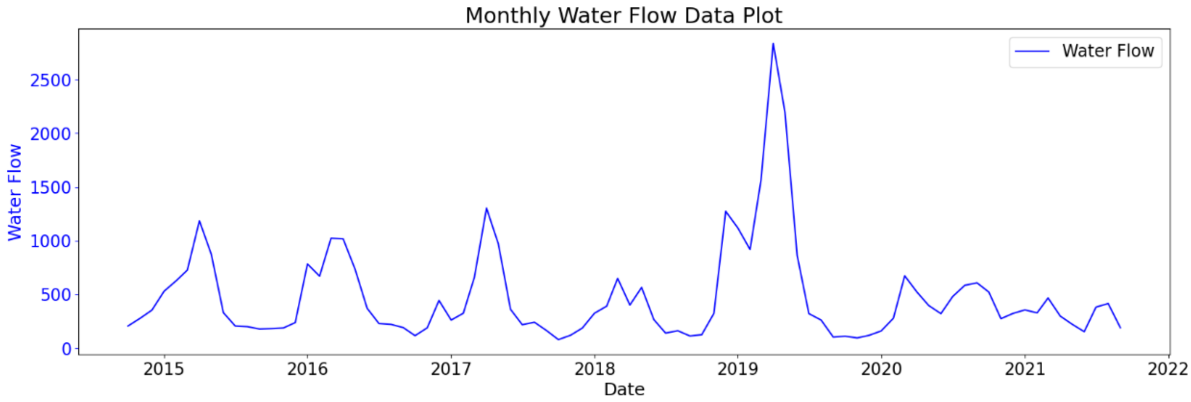

Figure 3. Time Series Behavior of Tigris Water Flow in Iraq from Oct. 2014 to Sep. 2021

Fig. 4 presents the data's distribution, which exhibits a positively skewed distribution. The tail extends to the right, with the majority of values concentrated at the lower values. The data follows a Log Pearson Type III distribution that can handle skewed data, which is widely used in hydrology and environmental statistics to model natural phenomena, such as river flows, flood frequency, rainfall, and extreme events.

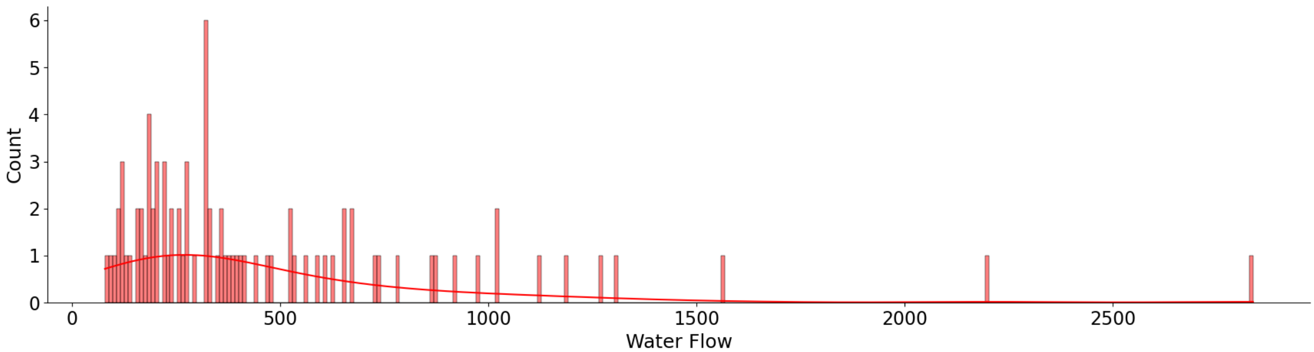

Figure 4. The distribution of the monthly time series of Tigris River flow in Iraq from Oct. 2014 to Sep. 2021

Fig. 5 illustrates the average monthly Tigris river flow for each month of the year. It reveals that March, April, and May experience the highest water flow, primarily due to precipitation seasonal conditions. In comparison, December, January, and February show lower water flow than March, April, and May, though they still exhibit higher flow than other months. The remaining months of the year demonstrate a consistent pattern with minimal variations, indicating that Tigris river flow does not significantly increase during these periods. This is due to the scarcity of rain during this period and the need for extensive water use.

Fig. 6 depicts the box plot of the data, which is a visualization of the data distribution based on five summary statistics: minimum, first quartile, median, third quartile, and maximum. It further detects outliers displayed as individual points outside the whiskers. The months from December to May show extreme values due to the yearly

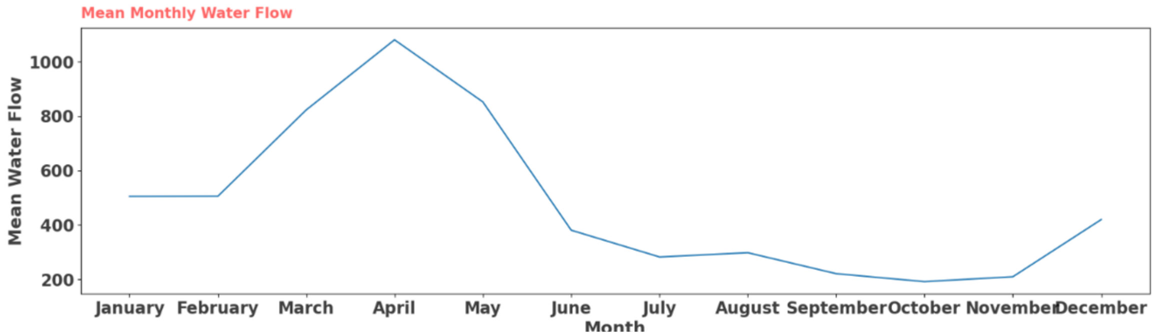

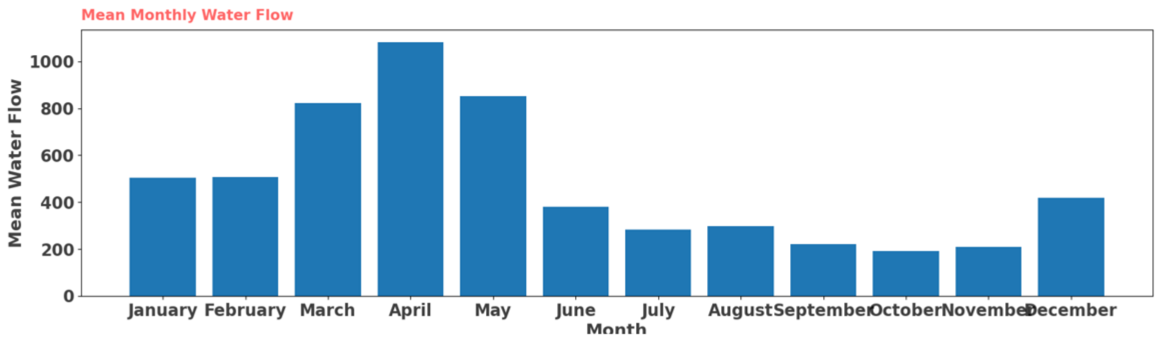

Figure 5. The average Tigris River flow for each month of the year in Iraq from Oct. 2014 to Sep. 2021.

precipitation season, which identifies the Tigris River in flow across different months and spots outliers in river flow. It can observe peak months, consistent river flow, and low-river flow periods.

Fig 7. demonstrates the four seasonal quarters (Q1, Q2, Q3, Q4), which display the monthly average of Tigris river flow over seasonal quarters and the confidence interval of 95% around the line to show the variability of the data. The data indicates that Tigris river flows are notably higher during the first and second quarters (Q1 and Q2). This trend is influenced by seasonal factors such as weather conditions and low water use during these periods. In contrast, Tigris River flow is significantly lower in the third and fourth quarters (Q3 and Q4), suggesting a decrease in Tigris River flow during these times. These observations highlight the need for water storage measures during the high river flow quarters (Q1 and Q2) to mitigate water seasonal quarters in the (Q3 and Q4) seasons.

Fig. 8 reveals the four stacked subplots (one for each component). Original time series data combines the effect of all components: trend, seasonality, and remainder (residuals). The trend represents long-term movements. The time series rose sharply in 2019, and then there was a significant and rapid decrease in the time series values around 2020. Then, the series shows a slight upward trend until med of 2020 and a more steady decline. A Seasonal plot depicts highlights repeating patterns over a year. The remainder captures fluctuations that are not explained by the trend and seasonality.

5. Models Used for Optimization and Forecasting

5.1. SARIMA Model

A forecast with the best ARIMA model was performed using the time series module in Minitab Statistical Software Version 22.1.0 to find the optimal model that minimizes the criteria (LogLikelihood, AIC, AICc, and BIC). The "Forecast with Best ARIMA Model" modeled the Tigris River flow data from Oct. 2014 to Dec. 2020. The SARIMA $(2, 1, 0) \times (5, 0, 1)_8$ (LogLikelihood = 9037.45, AIC = -18054.9, AICc = -18051.8, and BIC = -18030.7)

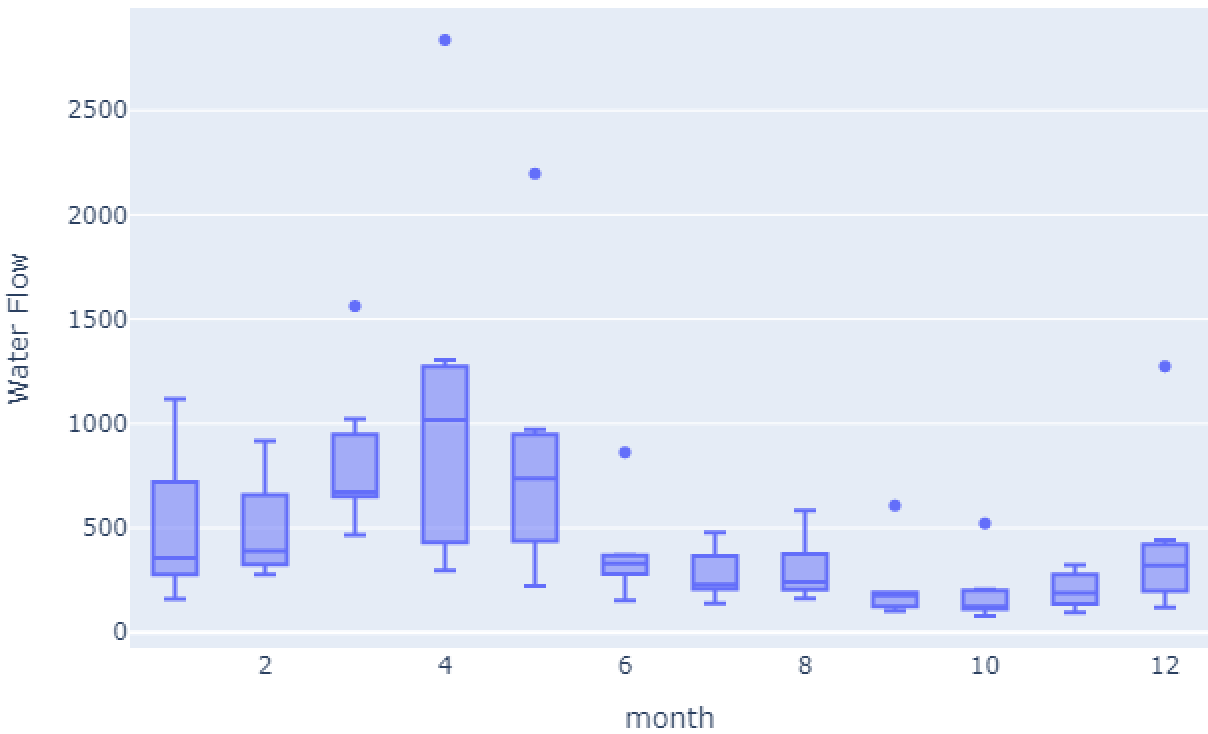

Figure 6. Box Plot of Tigris River flow in Iraq from Oct. 2014 to Sep. 2021

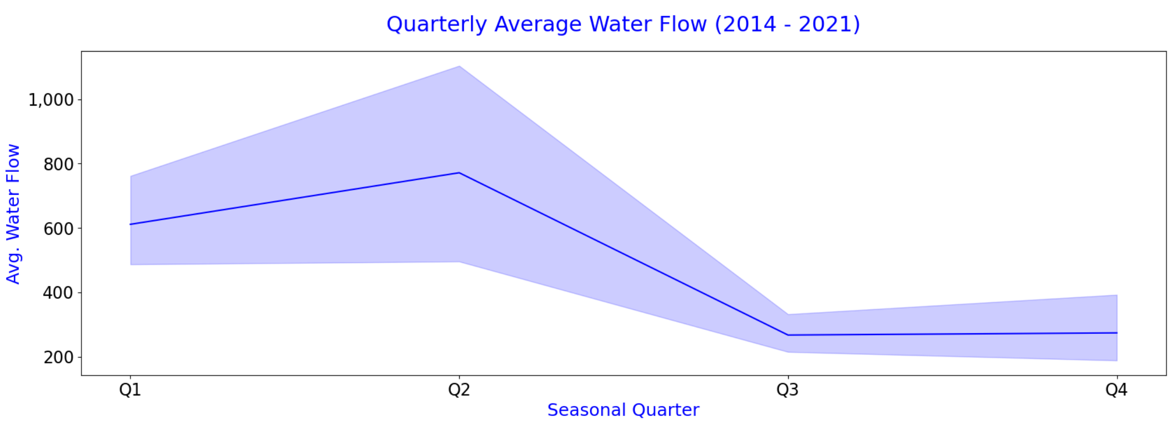

Figure 7. Quarterly Time Series of Tigris River flow in Iraq from Oct. 2014 to Sep. 2021

was the optimal model. Fig. 7 shows the Normal probability plot and the histogram for the prediction errors, normally distributed with a mean near zero. No significant autocorrelation or obvious pattern was identified in the residuals, which confirmed the normal distribution as shown in Fig. 9. The bars rising above or dropping below the dotted line revealed insignificant autocorrelation (P >0.05). Fig. 11 presents a comparison of actual and forecasted values. The forecasted values align with the actual data values.

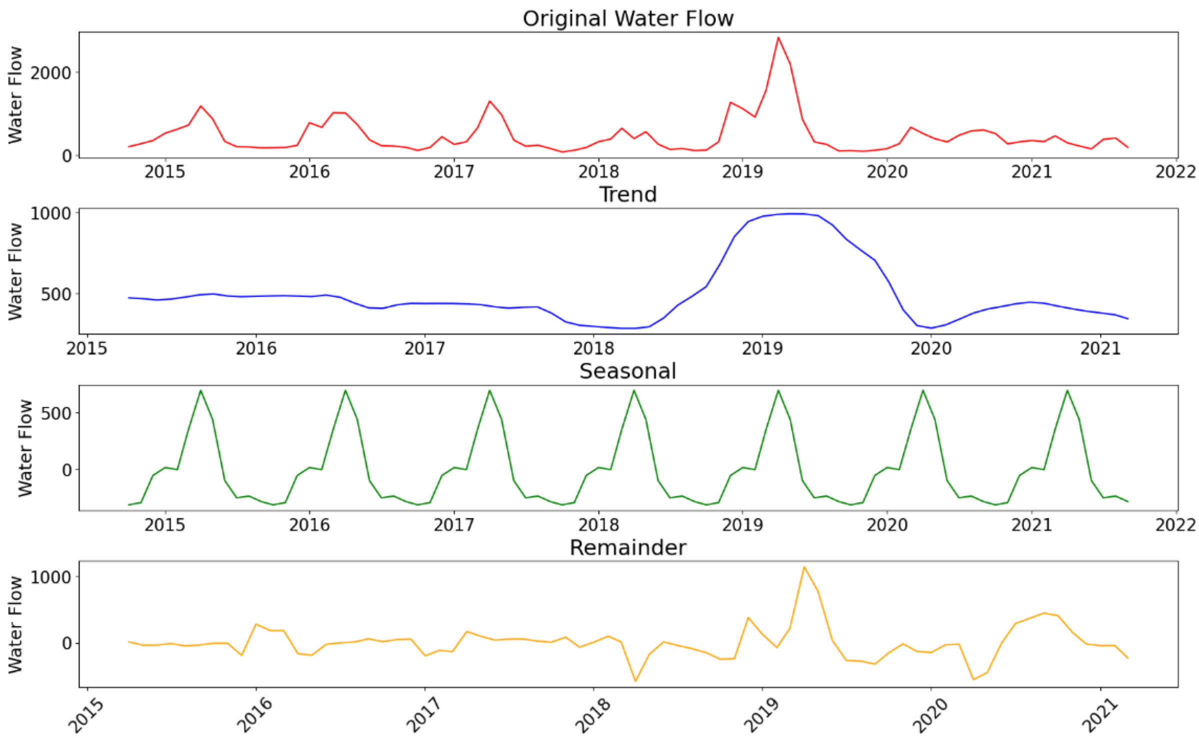

Figure 8. Decomposition of Monthly time series of Tigris River flow in Iraq from Oct. 2014 to Sep. 2021: Trend, Seasonal, and Remainder Components.

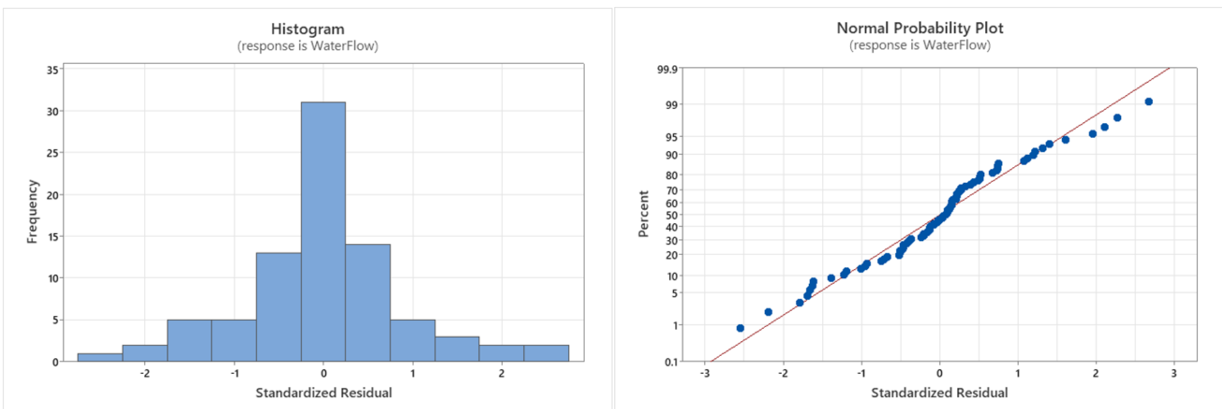

Figure 9. Histogram and Normal probability plot for the SARIMA $(2, 1, 0) \times (5, 0, 1)_8$ model prediction errors.

5.2. *ARIMAX Model*

Various traditional methods were evaluated to integrate external variables influencing the dependent series. We found that the most effective model was ARIMAX with the variables,the lagged value of the Tigris River flow at $t-1$, the lagged value of the Tigris River flow at $t-2$, the moving average of 2, MA(2), and the moving standard deviation of 2, MSD(2). The lagged variables were utilized to capture temporal dependencies, while the moving average was used to smooth short-term fluctuations and highlight trends. The model ARIMAX($p = 2, d = 1, q = 2, \mathbf{x} = (\text{lag1}, \text{lag2}, \text{MA}(2), \text{MSD}(2))$) effectively modeled the trends and fluctuations in the data. The

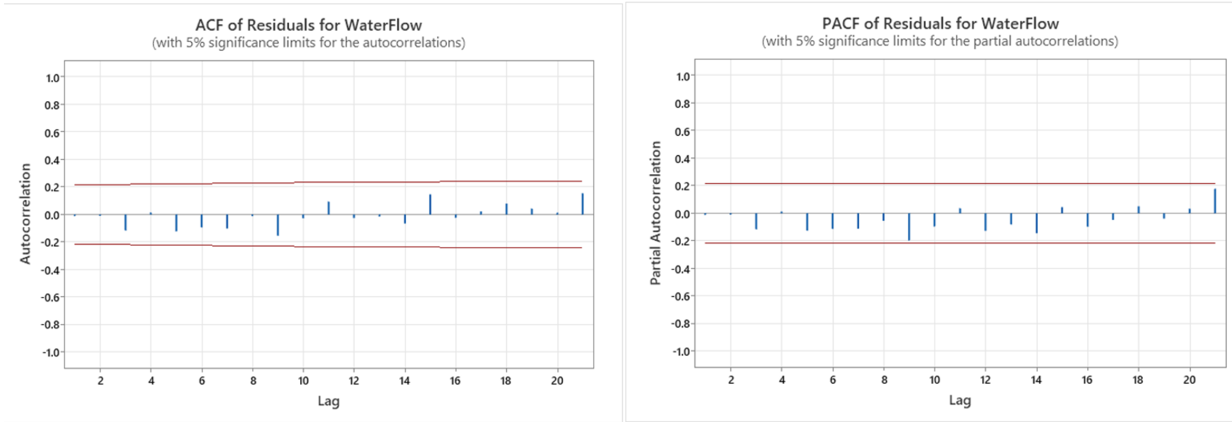

Figure 10. Autocorrelation (ACF) and Partial Autocorrelation (PACF) Plots for the Prediction Model SARIMA $(2,1,0) \times (5,0,1)_8$ of Tigris River Flow from Oct. 2014 to Dec. 2020.

model effectively captured underlying patterns and variations in the data, allowing for accurate forecasts. Fig (11) shows that the residuals are normally distributed. This indicates that the model's assumptions are met. Fig (12) shows the correlation diagnostics. No significant autocorrelation suggests that the model leaves no further patterns unexplained. Fig. 13 compares the actual and forecast values, where the model performance is clearly illustrated, as the forecasted values show a strong alignment with the actual data points, demonstrating a high degree of correctness and consistency in the predicted values.

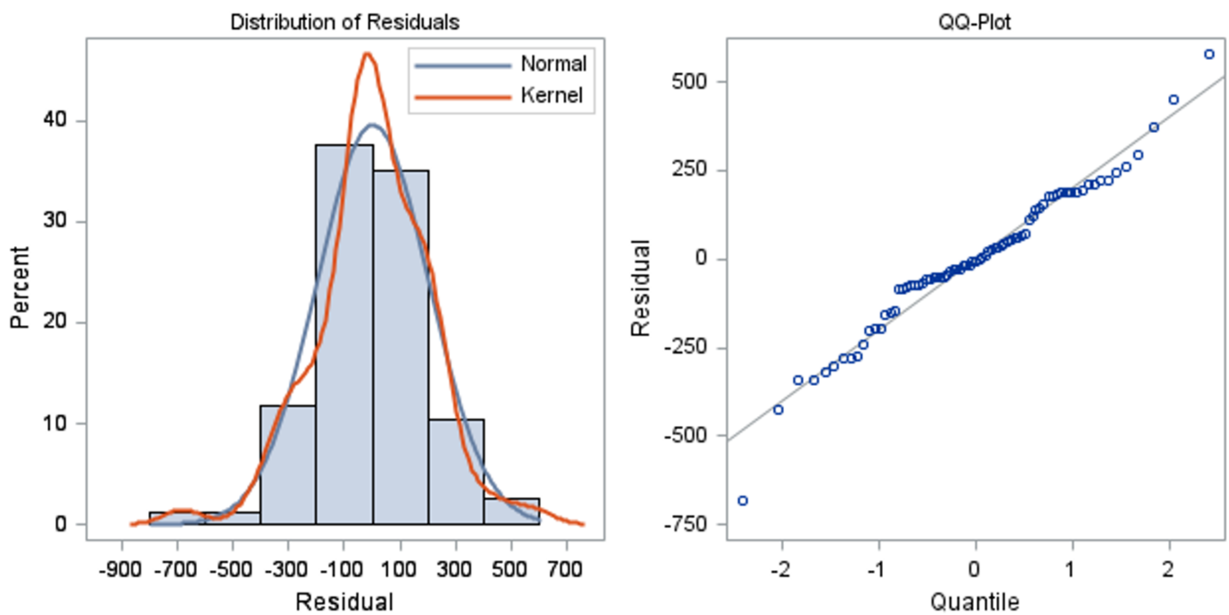

Figure 11. Residual Normality Diagnostics for the Prediction Model (ARIMAX(2,1,2)) of Tigris River Flow from Oct. 2014 to Dec. 2020.

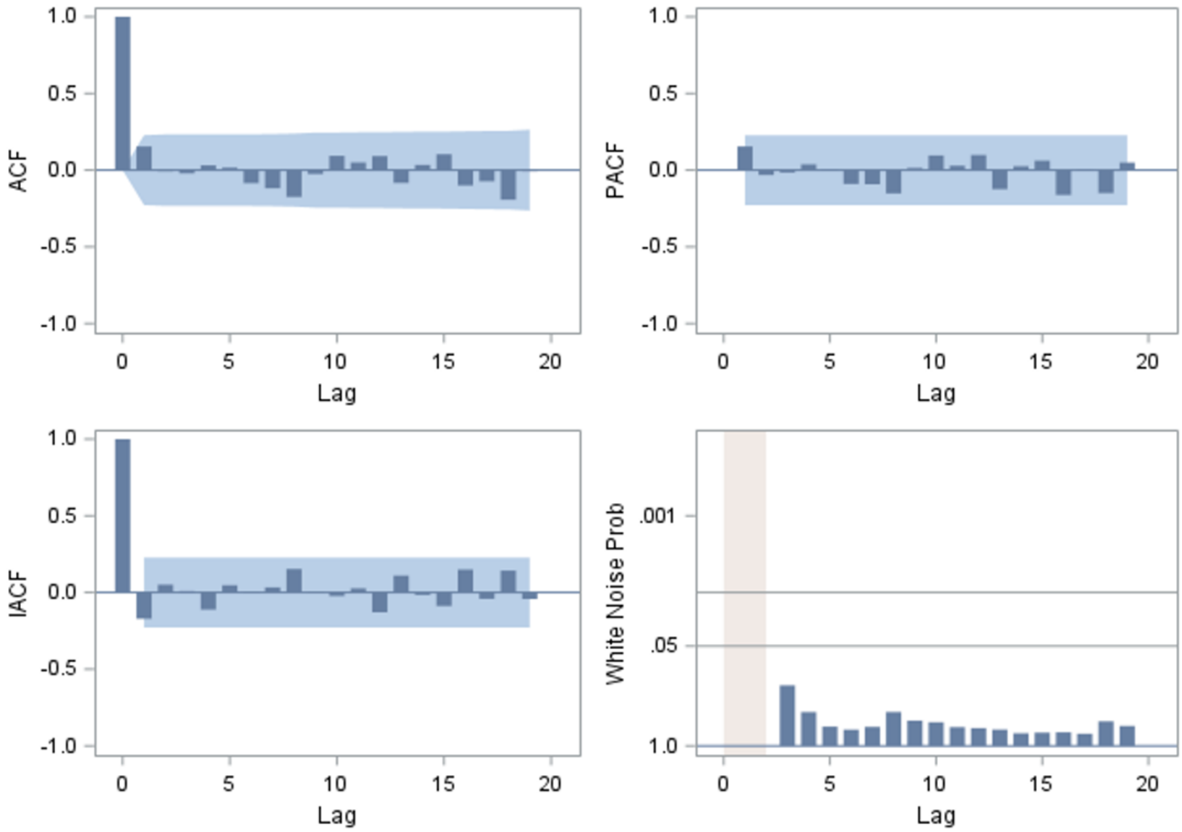

Figure 12. Residual Correlation Diagnostics for the Prediction Model (ARIMAX(2,1,2)) of Tigris River Flow from Oct. 2014 to Dec. 2020.

5.3. XGBoost regression model

Various machine-learning methods were explored. Each method was utilized and validated to identify the most effective technique for identifying and capturing the patterns in the data. After analysis and testing, the highest-performing model was found to be the XGBoost regression model with the four explanatory variables (Lag1, Lag2, MA(2), MSD(2)). XGBoost was configured and trained. Using the training data, we conducted a comprehensive grid search to identify the optimal parameters. Table (1) provides a detailed of search ranges for XGBoost hyperparameters.

Table 1. XGBoost Hyperparameter Search Ranges

Hyperparameter	**Search Ranges**
Max-depth	3-50
Minimum child weight	1-25
Gamma	0-25
Subsample	0.1-1
Learning rate	0.01-1
Colsample by tree	0.1-1
Alpha for L1 regularization	0-25
n_estimators	5-500

The optimal set of parameters that give the best model performance for the XGBoost model is as follows: "learning_rate" is 0.28; "min_child_weight" is 33; gamma is 12; "n_estimators" is 571, and "max_depth" is 18 levels. The contribution to model performance for the hyperparameter is as follows: the "learning_rate" at 0.43 and "min_child_weight" at 0.32 have the highest importance of hyperparameters in XGboost, while the importance decreases for gamma at 0.11, "n_estimators" at 0.09, and "max_depth" at 0.05.

Fig. 13 demonstrates the Tigris River flow for the testing data and showcases the actual values and the model's predicted values. The plot illustrates a close match between the actual and the predicted lines, reflecting a similar movement. This reveals the model's competence in capturing the latent patterns and temporal dependencies in the testing data, highlighting its effectiveness in providing precise predictions for the dataset.

5.4. Ensemble Model

Our study used an ensemble approach. The initial step involved identifying the optimal ARIMA forecasters by selecting and using an automatic framework from a broad range of combinations as a univariate model to analyze the intervention's impact. The second step included constructing an ARIMAX model as a multivariate time series model, linking the explanatory variables to the Tigris River flow to model interdependencies between variables. The third step included constructing an XGBoost model as a machine learning (ML) model, associating with the explanatory variables to the Tigris River flow to capture nonlinear relationships. Finally, to integrate and enhance the predictive outcomes of these methods, we combined the prediction of the best ARIMA models and XGBoost as inputs into a Random tree, enabling the assessment of Tigris River flow to produce the final forecast.

The forecast results for the SARIMA, ARIMAX, and XGBoost models were combined to produce the forecast results of the Random trees ensemble model. The optimal set of parameters that give the best model performance for the Random Trees Ensemble model is as follows: "n_estimators" is 145, "Maximum Depth" is 26; "Minimum Samples per Split" is 11; "Minimum Samples per Leaf" is 7, "Maximum Samples per Tree" is 2. "Maximum Features" is auto". From Fig. (13), it is observable that the forecasting results using the Random trees ensemble model demonstrate high potential in the context of Tigris River flow. The forecasts using the ensemble model are aligned with the actual and fit better than the ARIMAX, SARIMA, and XGBoost models, indicating the feasibility and effectiveness of the Random trees ensemble model. Furthermore, the forecasted Tigris River flow of the ensemble model changed the trend of the actual Tigris River flow. It matched the actual values well with the January to March 2019 peak. Demonstrated superior predictive accuracy and effectively accounted for fluctuations inherent in the Tigris River flow data, establishing it as the most suitable option for this study.

Figure (14) illustrates the performance of a Random Trees ensemble model applied to testing data from Jan 2020 to May 2021. The predicted values from the model are displayed alongside the actual observed data, highlighting the model's ability to reflect variations during the testing phase. The model accurately reflects key patterns, like prominent rises and falls, indicating strong performance.

Statistical metrics have been employed to assess the model's performance, providing valuable insights and complementary methods for forecast analysis and assessment. The RMSE, MAE, MAPE, R^2 and AIC of the SARIMA $(2,1,0) \times (5,0,1)_8$, ARIMAX, XGBoost, along with are Random Trees ensemble model presented in Table 1. The results highlight that the Random Trees ensemble model exhibits reliable forecasting accuracy and surpasses the performance of the SARIMA, ARIMA, and XGBoost models.

Table 2. Comparison of Forecasting Methods using Evaluation Metrics

Model	RMSE	MAE	MAPE	R^2	AIC
SARIMA	168.3	35.5	7.4	0.73	-98.38
ARIMAX	121.1	24.9	5.2	0.82	-107.46
XGBoost	77.9	17.7	3.7	0.88	-124.08
Random Trees ensemble model	53.7	13.4	2.8	0.92	-141.66

Figure (15) illustrates the prediction for the Tigris River flow in Iraq up to the Dec. year 2026. The projection indicates a noticeable increase in River flow starting in early 2022. Following this increase, the trend stabilizes,

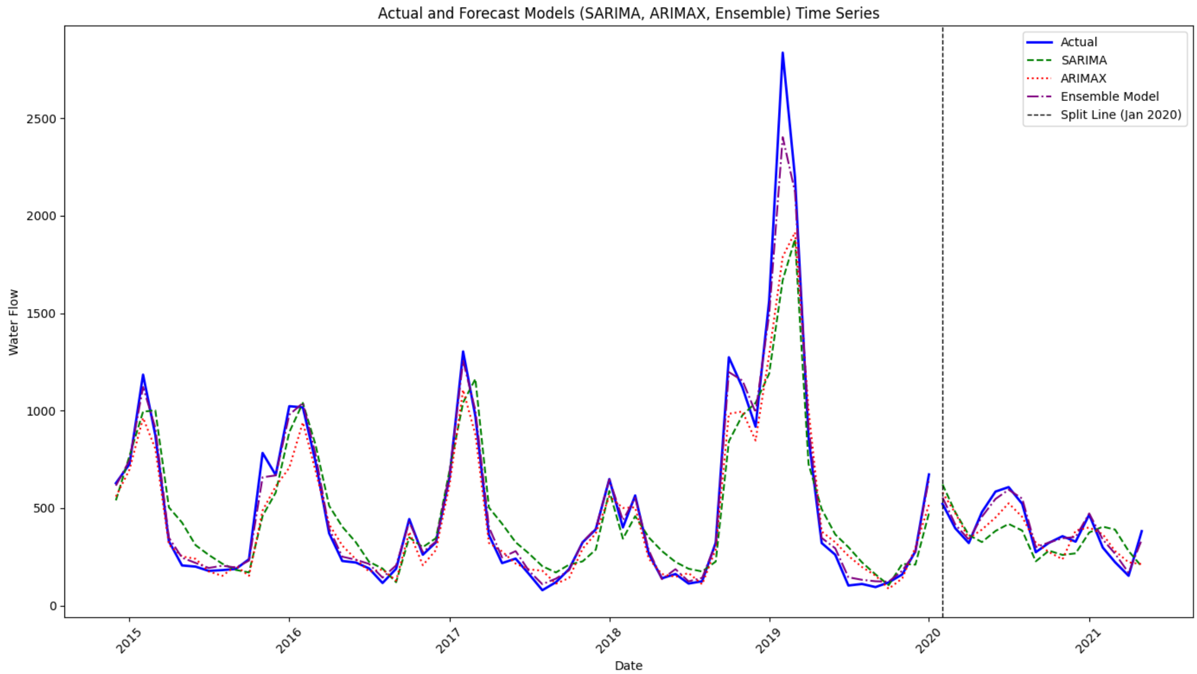

Figure 13. The forecast curves of the Random Trees ensemble model, SARIMA model, ARIMAX model, XGBoost model, and the Tigris River flow time series in Iraq (Oct. 2014 to May 2021). The forecasted values of the Random trees ensemble model demonstrated superior fitting accuracy over the SARIMA, ARIMAX, XGBoost models.

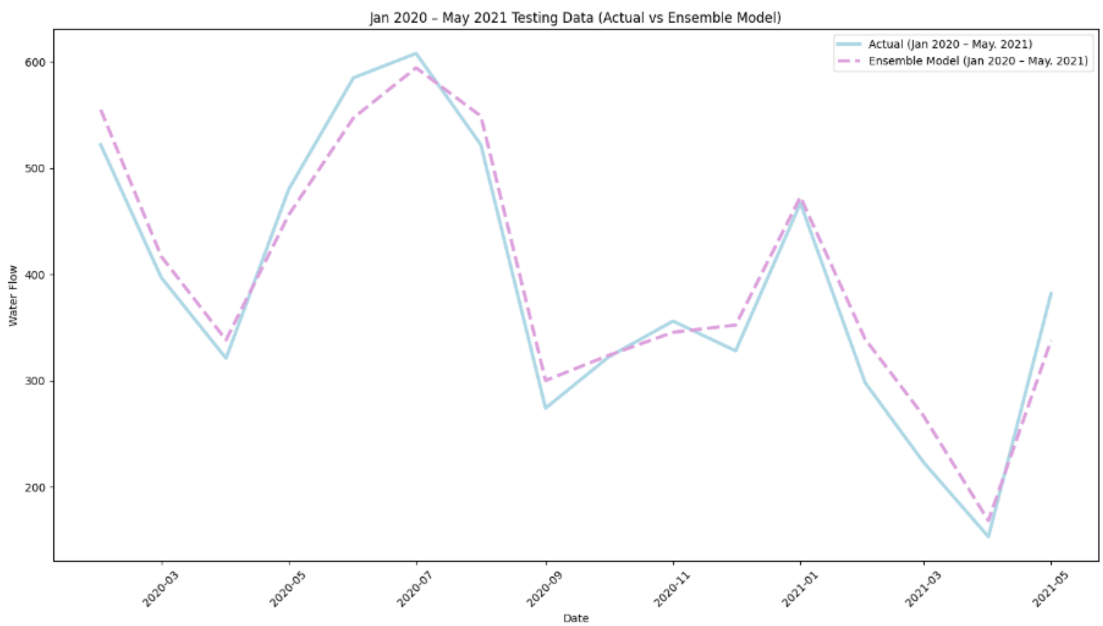

Figure 14. Forecasted vs. Actual Values for Testing Dataset for the Random Trees ensemble model for the Tigris River flow time series in Iraq.

aligning with the long-term average for river flow level with variations observed, particularly during the rainy season in Iraq and Turkey, where River flow varies based on the season. These seasonal changes reflect the impact of increased rainy season activity during peak times. Overall, the forecast suggests a stabilization of river flow until Oct. 2030.

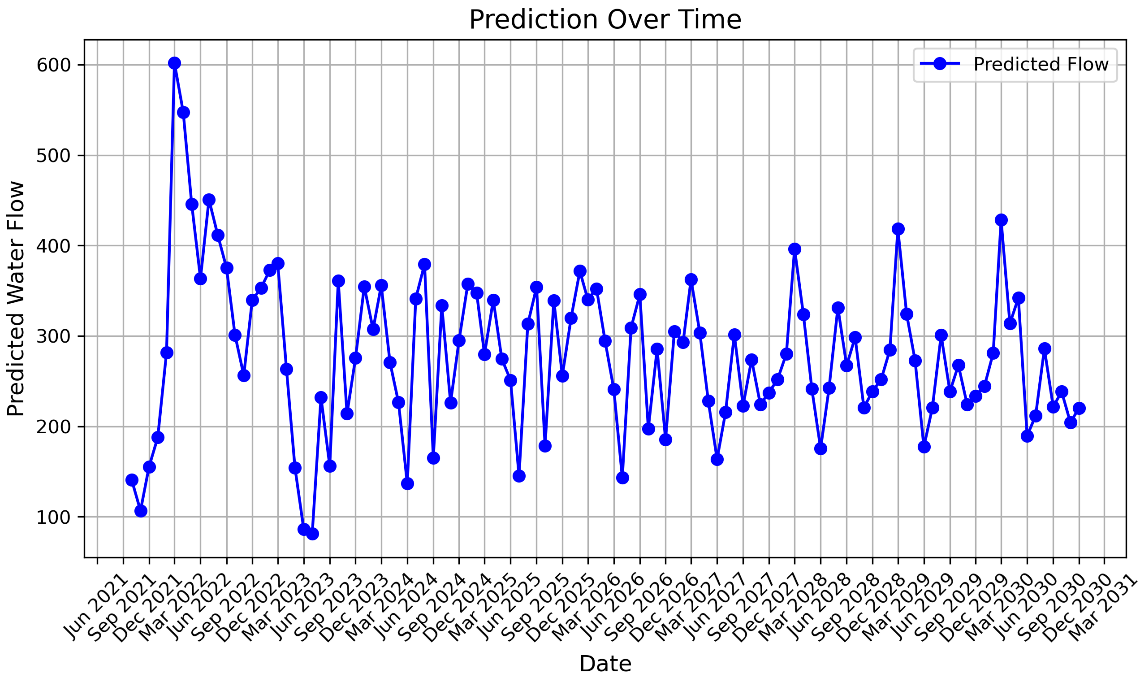

Figure 15. Projected Trends in Tigris River flow in Iraq (Oct. 2021–Oct. 2030).

Water plays a fundamental role in life-sustaining and vital availability. It is a primary challenge to national security. When scarce, it is a fundamental catalyst for conflicts, and its abundance brings prosperity and flourishing. It is essential in development, with the rising demand for this resource for sustained food availability and power generation. Therefore, extensive government measures to govern access to rivers and transboundary water sources are targeted at safeguarding their water resources. Environmental challenges such as climate change, drought, and land degradation are escalating, combined with human-driven threats represented by squandering, resource mismanagement, and pollution. Furthermore, unawareness about water's worth, with the belief that this resource is everlasting and replenishable. Some nations are also strategically controlling common resources through international pressure and economic blackmail. Reaching an agreement with Turkey on Iraq's water share requires collaboration through the sharing of information and technical knowledge. Conducting discussions, seeking advice, and creating a reliable framework based on mutual trust and promoting fair participation while upholding a commitment to protecting Iraq's water by adhering to the principle of equitable distribution, fostering cooperation with respect for sovereignty, and formulating a stable policy for shared river management. Moreover, establishing collaborative commercial projects and boosting inter-trade between basin countries, with the goal of achieving future partnerships, can mitigate tensions and contribute to shared economic growth.

6. Conclusion

The river flow system is the most vibrant and dynamic constituent, including linear and nonlinear components. Furthermore, its relationship with numerous variable factors is the most elaborate. So, predicting the results is highly challenging. This paper employed two distinct linear regression models to extract linear features, ARIMAX and SARIMA. While XGBoost of the nonlinear regression model was used to extract nonlinear features. Additive Regression with Random Trees ensemble is used to reach the conclusions. The analysis shows that the proposed method can significantly enhance the ability to forecast river flow, and it is an up-and-coming technique. The forecast suggests a stabilization of the river flow aligning with the low average river flow level, with variations observed. These seasonal changes reflect the impact of increased river flow during the rainy season in Iraq and Turkey during peak times and reduced river flow in the summer months.

REFERENCES

1. Central Statistical Organization, Directorate of Agricultural Statistics, *Water Resources Report 2019*, Iraq.
2. Ministry of Water Resources, Planning and Follow-up Department, Environmental Policies Division, *2023*.
3. I. E. Issa, N. Al-Ansari, G. Sherwany, and S. Knutsson, *Expected future of water resources within Tigris–Euphrates rivers basin, Iraq*, Journal of Water Resource and Protection, vol. 6, no. 5, pp. 421-432, 2014.
4. M. E. Mohammad, N. Al-Ansari, I. E. Issa, and S. Knutsson, *Sediment in Mosul Dam reservoir using the HEC-RAS model*, Lakes & Reservoirs: Research & Management, vol. 21, no. 3, pp. 235-244, 2016.
5. A. F. Farhan, K. K. Al-Ahmady, and N. A. A. Al-Masry, *Assessment of Tigris River water quality in Mosul for drinking and domestic use by applying CCME water quality index*, In *IOP Conference Series: Materials Science and Engineering*, vol. 737, no. 1, p. 012204, Feb. 2020, IOP Publishing.
6. A. T. Haghighi, M. Akbari, R. Noori, A. D. Mehr, A. Gohari, M. E. Sönmez, N. Abou Zaki, N. Yilmaz, and B. Kløve, *The impact of Turkey's water resources development on the flow regime of the Tigris River in Iraq*, Journal of Hydrology: Regional Studies, vol. 48, p. 101454, 2023.
7. M. C. Aydin, A. E. Ulu, and Ç. Karaduman, *CFD analysis of Ilısu Dam sluice outlet*, Turk. J. Sci. Technol., vol. 13, pp. 119–124, 2018.
8. M. Karalar and M. Çavuşli, *Effect of Normal and Shear Interaction Stiffnesses on Three-Dimensional Viscoplastic Creep Behaviour of a CFR Dam*, Advances in Civil Engineering, vol. 2018, no. 1, p. 2491652, 2018.
9. A. S. T. Al-Madhhachi, K. A. Rahi, and W. K. Leabi, *Hydrological impact of Ilisu dam on Mosul Dam; the river Tigris*, Geosciences, vol. 10, no. 4, p. 120, 2020.
10. K. A. Rahi and T. Halihan, *Salinity evolution of the Tigris River*, Regional Environmental Change, vol. 18, no. 7, pp. 2117–2127, 2018.
11. R. M. Adnan, X. Yuan, O. Kisi, and R. Anam, *Improving accuracy of river flow forecasting using LSSVR with gravitational search algorithm*, Advances in Meteorology, vol. 2017, no. 1, p. 2391621, 2017.
12. Q. Zhang, B. D. Wang, B. He, Y. Peng, and M. L. Ren, *Singular spectrum analysis and ARIMA hybrid model for annual runoff forecasting*, Water Resources Management, vol. 25, pp. 2683–2703, 2011.
13. J. Xu, Y. Chen, W. Li, Q. Nie, C. Song, and C. Wei, *Integrating wavelet analysis and BPANN to simulate the annual runoff with regional climate change: a case study of Yarkand River, Northwest China*, Water Resources Management, vol. 28, pp. 2523–2537, 2014.
14. I. F. Hasan and Y. N. Saeed, *Trend analysis of hydrological drought for selected rivers in Iraq*, Tikrit Journal of Engineering Sciences, vol. 27, no. 1, pp. 51-57, Mar. 2020.
15. X. Xu, Z. Wang, F. Zhou, Y. Huang, T. Zhong, and G. Trajcevski, *Dynamic transformer ODEs for large-scale reservoir inflow forecasting*, Knowledge-Based Systems, vol. 276, p. 110737, 2023.
16. Ö. Kişi, *River flow forecasting and estimation using different artificial neural network techniques*, Hydrology Research, vol. 39, no. 1, pp. 27–40, 2008.
17. H. R. Maier and G. C. Dandy, *The use of artificial neural networks for the prediction of water quality parameters*, Water Resources Research, vol. 32, no. 4, pp. 1013–1022, 1996.
18. D. Barrientos-Torres, E. A. Martinez-Ríos, S. A. Navarro-Tuch, J. L. Pablos-Hach, and R. Bustamante-Bello, *Water Flow Modeling and Forecast in a Water Branch of Mexico City through ARIMA and Transfer Function Models for Anomaly Detection*, Water, vol. 15, no. 15, p. 2792, 2023.
19. M. M. Al-Hashimi and H. A. Hayawi, *Nonlinear Model for Precipitation Forecasting in Northern Iraq using Machine Learning Algorithms*, Computer Science, vol. 19, no. 1, pp. 171-179, 2024.
20. D. M. Papamichail and P. E. Georgiou, *Seasonal ARIMA inflow models for reservoir sizing*, JAWRA Journal of the American Water Resources Association, vol. 37, no. 4, pp. 877–885, 2001.
21. M. R. Ghanbarpour, K. C. Abbaspour, G. Jalalvand, and G. A. Moghaddam, *Stochastic modeling of surface stream flow at different time scales: Sangsoorakh karst basin, Iran*, Journal of Cave and Karst Studies, vol. 72, no. 1, pp. 1–10, 2010.
22. M. Valipour, M. E. Banihabib, and S. M. R. Behbahani, *Comparison of the ARMA, ARIMA, and the autoregressive artificial neural network models in forecasting the monthly inflow of Dez dam reservoir*, Journal of Hydrology, vol. 476, pp. 433–441, 2013.
23. O. Bazrafshan, A. Salajegheh, J. Bazrafshan, M. Mahdavi, and A. Fatehi Maraj, *Hydrological drought forecasting using ARIMA models (case study: Karkheh Basin)*, Ecopersia, vol. 3, no. 3, pp. 1099–1117, 2015.
24. M. Valipour, *Long-term runoff study using SARIMA and ARIMA models in the United States*, Meteorological Applications, vol. 22, no. 3, pp. 592–598, 2015.
25. S. F. Ullah, Y. Zahra, and I. Hussain, *Time Series Forecasting with SARIMA Model of Water Outflow of Indus at Terbela River in Pakistan*, Bi-Annual Research Journal, vol. 44 (Special Edition), p. 349–379, 2019.
26. L. S. De Sousa, R. M. Wambua, J. M. Raude, and B. M. Mutua, *Water flow and sediment flux forecast in the Chókwè Irrigation Scheme, Mozambique*, Journal of Water Resource and Protection, vol. 12, no. 12, pp. 1089–1122, 2020.

27. M. A. Musarat, W. S. Alaloul, M. B. A. Rabbani, et al., *Kabul river flow prediction using automated ARIMA forecasting: A machine learning approach*, Sustainability, vol. 13, no. 19, p. 10720, 2021.
28. C. Pires and M. V. Martins, *Enhancing Water Management: A Comparative Analysis of Time Series Prediction Models for Distributed Water Flow in Supply Networks*, Water, vol. 16, no. 13, p. 1827, 2024.
29. M. Khashei, M. Bijari, and G. A. R. Ardali, *Improvement of auto-regressive integrated moving average models using fuzzy logic and artificial neural networks (ANNs)*, Neurocomputing, vol. 72, no. 4–6, pp. 956–967, 2009.
30. XiangJun Wang and M. M. Al-Hashimi, *The comparison of adaptive neuro-fuzzy inference system (ANFIS) with nonlinear regression for estimation and prediction*, in *2012 International Conference on Information Technology and e-Services*, Mar. 24, 2012, pp. 1–7, IEEE.
31. N. S. Roudbari, S. R. Punekar, Z. Patterson, U. Eicker, and C. Poullis, *From data to action in flood forecasting leveraging graph neural networks and digital twin visualization*, Scientific Reports, vol. 14, no. 1, p. 18571, 2024.
32. A. El-Shafie, M. R. Taha, and A. Noureldin, *A neuro-fuzzy model for inflow forecasting of the Nile River at Aswan high dam*, Water Resources Management, vol. 21, pp. 533–556, 2007.
33. W. Huang, B. Xu, and A. Chan-Hilton, *Forecasting flows in Apalachicola River using neural networks*, Hydrological Processes, vol. 18, no. 13, pp. 2545–2564, 2004.
34. A. Altunkaynak, *Forecasting surface water level fluctuations of Lake Van by artificial neural networks*, Water Resources Management, vol. 21, pp. 399–408, 2007.
35. C. L. Wu and K. W. Chau, *Data-driven models for monthly streamflow time series prediction*, Engineering Applications of Artificial Intelligence, vol. 23, no. 8, pp. 1350-1367, 2010.
36. A. Shabri and Suhartono, *Streamflow forecasting using least-squares support vector machines*, Hydrological Sciences Journal, vol. 57, no. 7, pp. 1275-1293, 2012.
37. A. M. Kalteh, *Monthly river flow forecasting using artificial neural network and support vector regression models coupled with wavelet transform*, Computers & Geosciences, vol. 54, pp. 1-8, 2013.
38. P. P. Bhagwat and R. Maity, *Hydroclimatic streamflow prediction using least square-support vector regression*, ISH Journal of Hydraulic Engineering, vol. 19, no. 3, pp. 320-328, 2013.
39. Z. He, X. Wen, H. Liu, and J. Du, *A comparative study of artificial neural network, adaptive neuro-fuzzy inference system and support vector machine for forecasting river flow in the semiarid mountain region*, Journal of Hydrology, vol. 509, pp. 379-386, 2014.
40. O. Kisi, B. Choubin, R. C. Deo, and Z. M. Yaseen, *Incorporating synoptic-scale climate signals for streamflow modelling over the Mediterranean region using machine learning models*, Hydrological Sciences Journal, vol. 64, no. 10, pp. 1240-1252, 2019.
41. F. Tosunoğlu, S. Hanay, E. Çintaş, and B. Özyer, *Monthly streamflow forecasting using machine learning*, Erzincan University Journal of Science and Technology, vol. 13, no. 3, pp. 1242-1251, 2020.
42. P. J. Sharma, P. L. Patel, and V. Jothiprakash, *Model tree technique for streamflow forecasting: a case study in sub-catchment of Tapi River Basin, India*, In Advances in Streamflow Forecasting, pp. 215-237, Elsevier, 2021.
43. S. J. Chebii, M. M. Mukolwe, and B. I. Ong'or, *River flow modelling for flood prediction using artificial neural network in ungauged Perkerra catchment, Baringo County, Kenya*, Water Practice & Technology, vol. 17, no. 4, pp. 914-929, 2022.
44. S. M. Reed, *An active learning convolutional neural network for predicting river flow in a human impacted system*, Frontiers in Water, vol. 5, p. 1271780, 2023.
45. R. Maiti, B. G. Menon, and A. Abraham, *Ensemble empirical mode decomposition based deep learning models for forecasting river flow time series*, Expert Systems with Applications, vol. 255, p. 124550, 2024.
46. K. Wang, S. S. Band, R. Ameri, M. Biyari, T. Hai, C. C. Hsu, M. Hadjouni, H. Elmannai, K. W. Chau, and A. Mosavi, *Performance improvement of machine learning models via wavelet theory in estimating monthly river streamflow*, Engineering Applications of Computational Fluid Mechanics, vol. 16, no. 1, pp. 1833-1848, 2022.
47. N. J. Ibrahim and H. A. A. Hayawi, *Employment the State Space and Kalman Filter Using ARMA models*, IJASEIT, vol. 11, no. 1, pp. 145-149, 2021.
48. H. A. Hayawi and N. S. Alsharabi, *Analysis of multivariate time series for some linear models by using multi-dimensional wavelet shrinkage*, Periodicals of Engineering and Natural Sciences, vol. 10, no. 4, pp. 120-129, Jul. 2022.
49. M. M. Al-Hashimi, H. A. Hayawi, and M. Al-Kassab, *A Comparative Study of Traditional Methods and Hybridization for Predicting Non-Stationary Sunspot Time Series*, Computer Science, vol. 19, no. 1, pp. 195-203, 2024.
50. G. E. Box and G. C. Tiao, *Intervention analysis with applications to economic and environmental problems*, Journal of the American Statistical Association, vol. 70, no. 349, pp. 70-79, 1975.
51. T. Chen and C. Guestrin, *Xgboost: A scalable tree boosting system*, In Proceedings of the 22nd ACM SIGKDD International Conference on Knowledge Discovery and Data Mining, pp. 785-794, 2016.
52. W. Ma, X. Zhang, J. Xie, G. Zuo, F. Luo, X. Zhang, T. Jin, and X. Yang, *Prediction of non-stationary daily streamflow series based on ensemble learning: a case study of the Wei River Basin, China*, Stochastic Environmental Research and Risk Assessment, pp. 1-21, 2024.
53. L. Ni, D. Wang, J. Wu, Y. Wang, Y. Tao, J. Zhang, and J. Liu, *Streamflow forecasting using extreme gradient boosting model coupled with Gaussian mixture model*, Journal of Hydrology, vol. 586, p. 124901, 2020.
54. J. Luo, Z. Zhang, Y. Fu, and F. Rao, *Time series prediction of COVID-19 transmission in America using LSTM and XGBoost algorithms*, Results in Physics, vol. 27, p. 104462, 2021.
55. H. Wu and D. Levinson, *The ensemble approach to forecasting: A review and synthesis*, Transportation Research Part C: Emerging Technologies, vol. 132, p. 103357, 2021.
56. H. Allende and C. Valle, *Ensemble methods for time series forecasting*, Claudio Moraga: A Passion for Multi-Valued Logic and Soft Computing, pp. 217-232, 2017.
57. M. H. D. M. Ribeiro and L. dos Santos Coelho, *Ensemble approach based on bagging, boosting and stacking for short-term prediction in agribusiness time series*, Applied Soft Computing, vol. 86, p. 105837, 2020.
58. S. Kalmegh, *Analysis of Weka data mining algorithm Reptree, Simple CART, and RandomTree for classification of Indian news*, International Journal of Innovative Science, Engineering & Technology, vol. 2, no. 2, pp. 438-446, 2015.

59. M. K. Khan and M. K. Jindal, *Random tree algorithm to analyse the relation between type of traumatic dental injuries and its demographic and predisposing factors—a cross-sectional study*, Indian Journal of Dental Research, vol. 34, no. 2, pp. 114-118, 2023.
60. R. Assaad and I. H. El-Adaway, *Bridge infrastructure asset management system: Comparative computational machine learning approach for evaluating and predicting deck deterioration conditions*, Journal of Infrastructure Systems, vol. 26, no. 3, p. 04020032, 2020.
61. A. Rashidi Nasab and H. Elzarka, *Optimizing machine learning algorithms for improving prediction of bridge deck deterioration: A case study of Ohio bridges*, Buildings, vol. 13, no. 6, p. 1517, 2023.
62. S. Ramya, S. Srinath, and P. Tuppad, *Comprehensive analysis of multiple classifiers for enhanced river water quality monitoring with explainable AI*, Case Studies in Chemical and Environmental Engineering, vol. 10, p. 100822, 2024.
63. B. Liu, H. Wen, M. Di, J. Huang, M. Liao, J. Yu, and Y. Xiang, *Mapping and interpretability of aftershock hazards using hybrid machine learning algorithms*, Journal of Rock Mechanics and Geotechnical Engineering, 2024.
64. V. Markovtsev, W. Long, H. Mougard, K. Slavnov, and E. Bulychev, *STYLE-ANALYZER: fixing code style inconsistencies with interpretable unsupervised algorithms*, In *2019 IEEE/ACM 16th International Conference on Mining Software Repositories (MSR)*, pp. 468-478, IEEE, May 2019.